Friction Mechanisms of Silicon Wafer and Silicon Wafer Coated with Diamond-like Carbon Film and Two Monolayers

R. Arvind Singh, Eui-Sung Yoon*, Hung-Gu Han and Hosung Kong
Tribology Research Center, Korea Institute of Science and Technology, Seoul 130-650, Korea

The friction behaviour of Si-wafer, diamond-like carbon (DLC) and two self-assembled monolayers (SAMs) namely dimethyldichlorosilane (DMDC) and diphenyl-dichlorosilane (DPDC) coated on Si-wafer was studied under loading conditions in milli-newton (mN) range. Experiments were performed using a ball-on-flat type reciprocating micro-tribo tester. Glass balls with various radii 0.25 mm, 0.5 mm and 1 mm were used. The applied normal load was in the range of 1.5 mN to 4.8 mN. Results showed that the friction increased with the applied normal load in the case of all the test materials. It was also observed that friction was affected by the ball size. Friction increased with the increase in the ball size in the case of Si-wafer. The SAMs also showed a similar trend, but had lower values of friction than those of Si-wafer. Interestingly, for DLC it was observed that friction decreased with the increase in the ball size. This distinct difference in the behavior of friction in DLC was attributed to the difference in the operating mechanism. It was observed that Si-wafer and DLC exhibited wear, whereas wear was absent in the SAMs. Observations showed that solid-solid adhesion was dominant in Si-wafer, while plowing in DLC. The wear in these two materials significantly influenced their friction. In the case of SAMs their friction behaviour was largely influenced by the nature of their molecular chains.

Key Words : Friction, Wear, Tribology, DLC, SAM

1. Introduction

Engineering of surfaces has emerged as a novel solution for various tribological requirements, especially at nano/micro-scales. During the last decade, the advent of micro-electro-mechanical systems (MEMS) (Bhushan, 2001a) and high-density magnetic recording media (Komvopoulos, 2000) have promoted investigations directed towards enhancing the tribological performance of surfaces in contact at these scales. At these scales as sizes shrink from 1 mm to 1 micron, while the area decreases only by a factor of a million, the volume decreases by a factor of a billion (URL : http ://www.eetimes.com). Thus, as size shrinks, surface forces such as adhesion, meniscus forces and friction become 1000 times more influential merely because of the area to volume ratio is very high (a ratio of 1000) (URL: http://www.eetimes.com). In devices such as MEMS, lateral and vertical gaps (clearances) between components are just around 1 μm (Maboudian et al., 1997) and thus conventional liquid lubricants cannot be used, as they would cause liquid-mediated adhesion leading to high static friction (Bhushan, 2001b). Hence, during sliding, in addition to the frictional effects due to external load, friction arising due to the intrinsic liquid-mediated adhesive force also needs to be overcome. Under such circumstances, tribological solutions to minimize friction and wear assume prime importance. Traditionally, silicon is the

* Corresponding Author,
E-mail : esyoon@kist.re.kr
TEL : +82-2-958-5651; **FAX** : +82-2-958-5659
Tribology Research Center, Korea Institute of Science and Technology, Seoul 130-650, Korea. (Manuscript **Received** July 13, 2005; **Revised** March 8, 2006)

widely used material for the fabrication of MEMS devices and hence, most of the investigations have been directed towards enhancing its tribological performance (Bhushan, 2001a, 2001b). In the past, several investigations that were focused on improving the tribological behaviour of silicon, have led to the development of various surface modification techniques such as chemical modification (Maboudian et al., 1997; Bhushan, 2001b) and topographical modification (Bhushan, 1999; Ando et al., 1997). Topographical modification includes laser texturing (Bhushan, 1999) and micro-dimple formation (Ando et al., 1997). Amongst the various chemical modification techniques, self-assembled monolayers (SAMs) and diamond-like carbon (DLC) coatings are the most promising treatments. Several authors have earlier reported significant improvement in the nano/micro-scale tribological behaviour of silicon coated with SAMs and DLC (Sundararajan et al., 1999; Yoon et al., 2003; Liu et al., 2001; Ahmed et al., 1999). As for the real time application of these coatings, SAMs have found their role as lubricants in micro-motors (Maboudian et al., 2004) and digital micromirrors (Henck, 1997), while DLC coatings are being increasingly used in magnetic recording heads (Sundararajan et al., 1999).

In the present work, the friction behaviour of Si-wafer (100), DLC and two self-assembled monolayers namely dimethyldichlorosilane (DMDC) and diphenyl-dichlorosilane (DPDC) coated on Si-wafers has been investigated experimentally under loading conditions in milli-newton (mN) range. The underlying mechanisms that affect the friction behaviour in these test samples have been reported in this paper.

2. Experimental

2.1 Test specimens

Soda Lime balls (Duke Scientific Corporation) with radii 0.25 mm, 0.5 mm and 1 mm were used for the study of friction. The test materials were Si-wafer ((100), produced by LG Siltron), DLC film and dimethyldichlorosilane (DMDC) and diphenyldichlorosilane (DPDC) coated on Si-wafers (100). All experiments were conducted at controlled conditions of temperature (24±1℃) and relative humidity (45±5%). Si-wafer (100) samples of 10 mm×10 mm were cut from the as-received discs using a diamond tip cutter and were cleaned with blowing air using a hand-blower. The DLC films were deposited by a radio frequency plasma-assisted chemical vapor deposition method (r.f.PACVD) using benzene (C_6H_6) as a reaction gas. Details of the experimental set up were described elsewhere (Lee et al., 1995). The deposition time was adjusted to obtain about 1 μm thick film. The film thickness was measured by an Alpha-step (Tencor P-1). The structure and mechanical properties of the deposited DLC films have been reported previously (Lee et al., 1995). The SAMs were coated on Si-wafer using the chemical vapor deposition (CVD) technique (Oh et al., 2004; Singh et al., 2005). Table 1 shows the properties of the ball material and test specimens used in the present study. The data on the elastic modulus, Poisson's ratio and interfacial energy are referred from various sources (Lee et al., 1995; Grischke et al., 1998; Sundararajan et al., 2001; Matweb, Scherge et al., 2001). The water contact angle of the test speci-

Table 1 Properties of ball material and test specimens

Material	Young's Modulus (GPa)	Poisson's Ratio	Water Contact Angle (Degrees)	Interfacial Energy (mN/m)
Soda Lime Glass	68	0.16	–	–
Si-wafer	165	0.28	22	72
DLC	120	0.26	66	41.3
DMDC-SAM	–	–	103	–
DPDC-SAM	–	–	84	–

mens were measured experimentally using sessile drop method. The water contact angles have been measured more than five times and the average values have been mentioned in Table 1.

2.2 Test apparatus

Figure 1 shows the ball-on-flat type reciprocating micro-tribotester. This tester was specifically designed so that it bridges the performance gap between nanoprobes and macrotribotesters. Friction was measured at the applied normal loads of 1.5 mN, 3.0 mN and 4.8 mN against glass balls of 0.25 mm, 0.5 mm and 1 mm radii. The sliding speed and the scan length were kept constant at 1 mm/sec and 3 mm respectively. Tests were repeated more than three times and the average values were plotted. Evidences of operating mechanisms in the test samples were obtained using Scanning Electron Microscope (SEM) and Atomic Force Microscope (AFM).

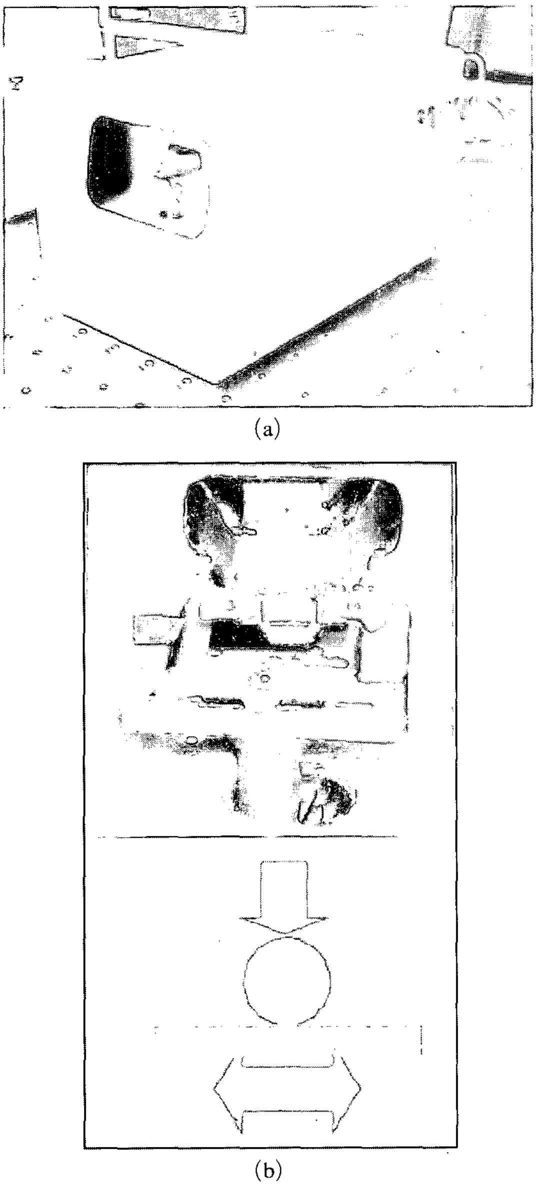

(a) (b)

Fig. 1 (a) Reciprocating type microtribotester and (b) a close-up view of the ball-on-flat configuration

3. Results and Discussion

Figures 2 and 3 show the variation of coefficient of friction as a function of applied normal load for various ball sizes in Si-wafer and DLC respectively. The coefficient of friction was estimated as the ratio of measured friction force to the applied normal load. The coefficient of friction in the case of Si-wafer increases with the ball

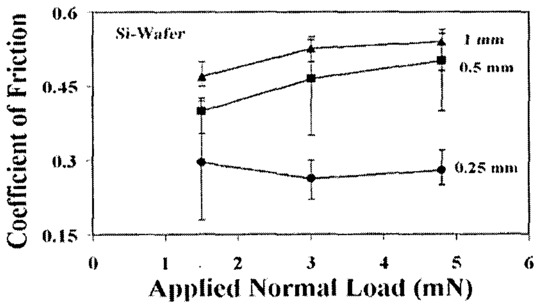

Fig. 2 Coefficient of friction in Si-wafer as a function of applied normal load

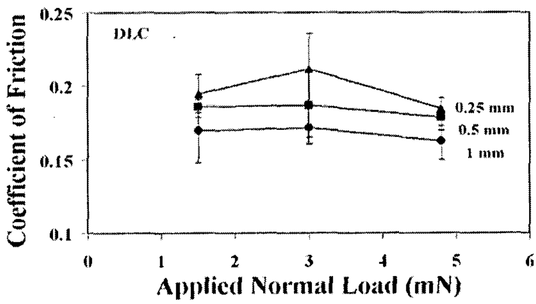

Fig. 3 Coefficient of friction in DLC as a function of applied normal load

size (Fig. 2), while it had an inverse relation in DLC (Fig. 3). Figs. 4 and 5 show the values of coefficient of friction of that of DMDC SAM and DPDC SAM respectively. In the case of the SAMs the coefficient of friction increased with the ball size. From the Fig. 2 to Fig. 5 it could be seen that Si-wafer shows highest values of coefficient of friction when compared with the rest of the test materials. In order to understand the friction behaviour in these materials i.e. to identify the operating mechanisms, microscopic analysis of surfaces after the tests was conducted. Evidences obtained showed that Si-wafer and DLC exhibited wear, whereas wear was absent in both of the SAMs.

Figure 6 shows the worn surfaces of Si-wafer tested at the following conditions of ball size and applied normal load : (a) 0.25 mm, 3 mN, Si-wafer, (b) 0.5 mm, 3 mN, Si-wafer and (c) 1 mm, 3 mN, Si-wafer, respectively. It could be observed that the width of the wear track increases with the ball size. Further, wear debris were found smeared on these tracks. These microscopic evidences clearly indicate that solid-solid adhesion

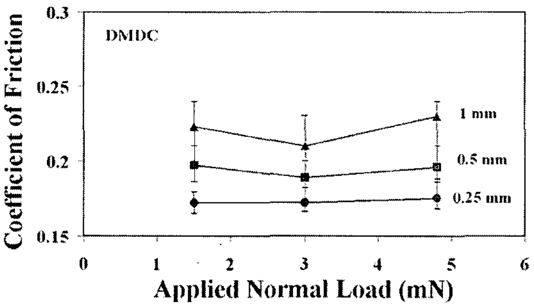

Fig. 4 Coefficient of friction of DMDC SAM as a function of applied normal load

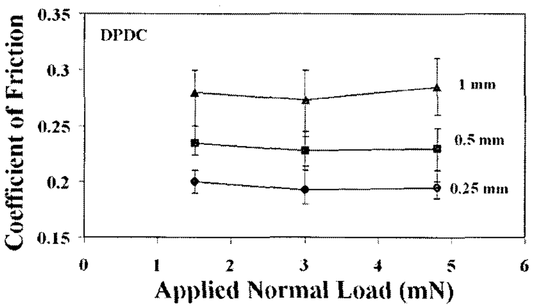

Fig. 5 Coefficient of friction of DPDC SAM as a function of applied normal load

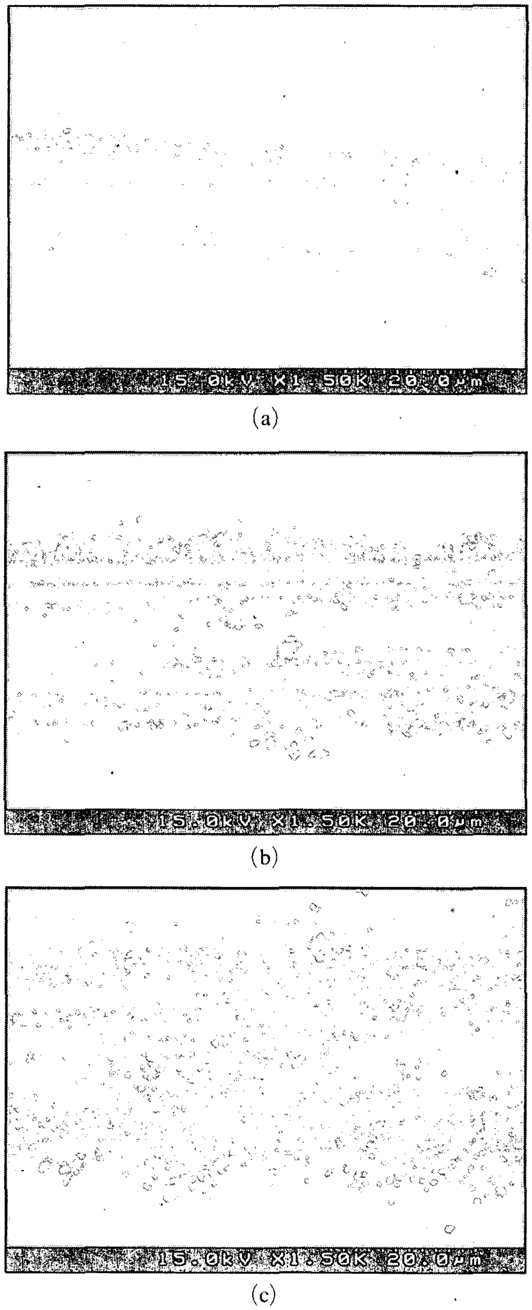

Fig. 6 SEM images of worn surfaces of Si-wafer tested at the following conditions of ball size and applied normal load respectively : (a) 0.25 mm, 3 mN, Si-wafer, (b) 0.5 mm, 3 mN, Si-wafer, (c) 1 mm, 3 mN, Si-wafer

was prominent in Si-wafer, which influenced its friction. The occurrence of solid-solid adhesion in Si-wafer was due to its high interfacial energy (Table 1). In the past, experiments conducted by Gardos (1996) showed that Si-wafer exhibits a high adhesive friction followed by shear-induced microcracking in the wake of the sliding contact.

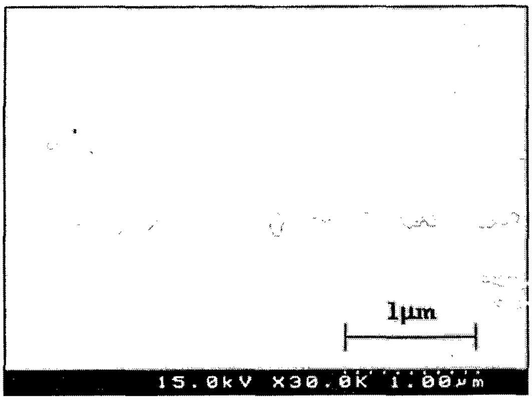

(a)

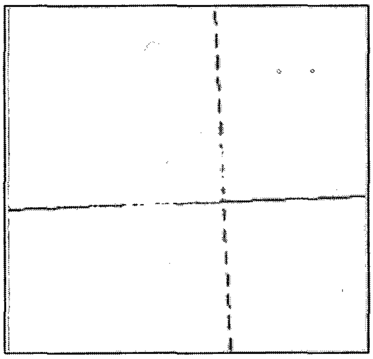

(b)

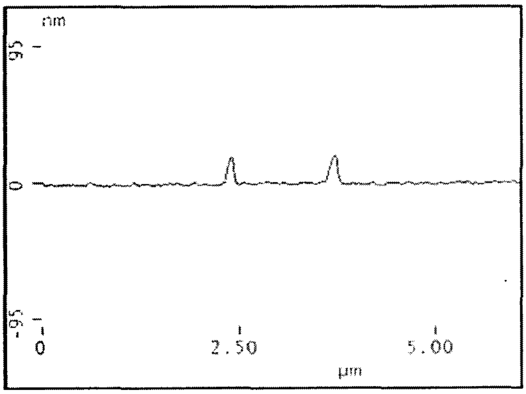

(c)

Fig. 7 (a) SEM image of the wear track in DLC against the glass ball of 0.25 mm radius at 3 mN normal load, (b) AFM image of the wear track in DLC and (c) cross-sectional profile of the wear track

Figure 7(a) is a high magnification SEM micrograph of the wear track in DLC that was tested against the glass ball of 0.25 mm radius at 3 mN normal load. The wear track shows evidences of plowing and plastic deformation. Wear debris are absent on the wear track. Fig. 7(b) shows the AFM image of the wear track (Fig. 7(a)) and Fig. 7(c) shows the cross-sectional profile of the wear track taken using the AFM. The profile has two peaks, which correspond to the ridges (material flow) formed along the wear track due to the plowing effect. These evidences indicate that 'plowing' was the dominant operating mechanism, which largely influenced the friction in DLC. Formation of transfer film followed by interfilm sliding has been reported earlier in DLC coatings (Bhushan, 2001b; Eun et al., 1996; Yoon et al., 1998). Under such circumstances, wear occurs at the transfer layer and the material gets removed in the form of rolled debris (Eun et al., 1996; Yoon et al., 1998). Further, it is important to note that the testing conditions under which DLC exhibited transfer layer formation (Eun et al., 1996; Yoon et al., 1998) were more aggressive than the present experimental conditions. Fig. 8 (a) shows rolled debris formed at the wear track in a DLC coating that was tested at conditions more severe than the present (Yoon et al., 1998). Fig. 8(b) shows an enlarged micrograph of rolled debris (Yoon et al., 1998). From the evidences obtained in the present work (Fig. 7), the absence of rolled wear debris at the wear track indicate that there has been no formation of tribo-layer, rather the evidences indicate that 'plowing' was the dominant mechanism in DLC. Fig. 9(a) shows SEM image of the ball surface (radius of 0.5 mm) tested against Si-wafer at 3.0 mN normal load, which shows debris sticking at the tip of the ball surface. Fig. 9(b) is a SEM image of the ball surface (radius 0.25 mm) tested against DLC at 3.0 mN normal load, which shows counterface material stacked at the tip of the ball surface (absence of compaction, but uneven stacking of

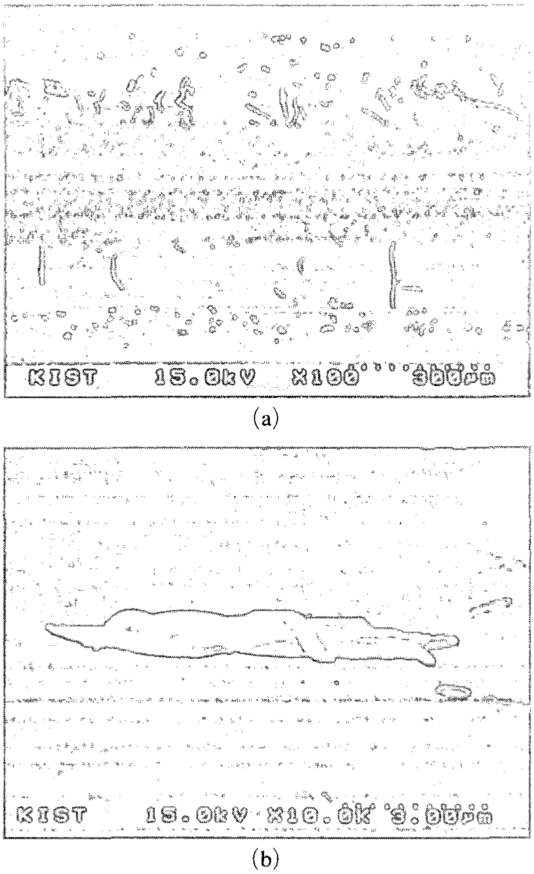

Fig. 8 (a) SEM micrograph of wear track of DLC coated on Si (100) wafer, tested against a steel ball of diameter 12.7 mm (4.9 N normal load, 0.05 m/s sliding speed) and (b) an enlarged micrograph of rolled debris (Yoon et al, 1998)

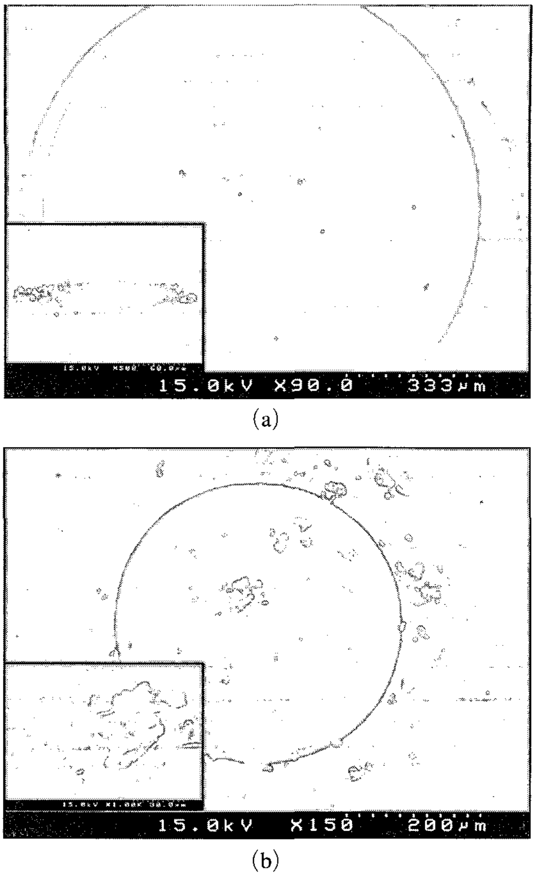

Fig. 9 (a) SEM image of the ball surface (radius of 0.5 mm) tested against Si-wafer at 3.0 mN normal load and (b) SEM image of the ball surface (radius 0.25 mm) tested against DLC at 3.0 mN normal load. In both these figures the insets show the respective ball surfaces at higher magnifications

material on the tip of the ball). In both these figures the insets show the respective ball surfaces at higher magnifications. From these figures it is further evident that the material removal (wear) in the case of Si-wafer and DLC has been distinctly different. They clearly indicate that solid-solid adhesion was prominent in Si-wafer, whereas DLC showed plowing. In both these materials (Si-wafer and DLC) wear influenced their friction. Unlike in the case of Si- wafer and DLC, the SAMs did not exhibit any wear.

As mentioned above, Si-wafer exhibits solid-solid adhesion. In this case, the contact area directly affects the mechanism and increases the friction force, which is in accordance with the fundamental law of adhesive friction given by Bowden and Tabor (1950). According to the theory proposed by Bowden and Tabor (1950), the real area of contact directly affects friction force in the case of a single asperity contact. Equation (1) gives the expression for the friction force.

$$F_f = \tau A_r \tag{1}$$

where, τ is the shear strength, an interfacial property and Ar the real area of contact.

Further, the contact area depends on the applied normal load and the ball size as per the

Johnson-Kendall-Roberts (JKR) model (Johnson et al., 1971). According to this model, the contact area is related to the applied normal load, the ball size and the interfacial energy of a material as given in equation (2).

$$A_r=\pi[R/K(F_n+6\pi\gamma R+[12\pi\gamma R\ F_n+(6\pi\gamma R)^2]^{1/2})]^{2/3} \quad (2)$$

where, R is the size of the ball, K the effective elastic modulus, F_n the applied normal load and γ, the interfacial energy of the material. This explains for the increase in coefficient of friction of Si-wafer with the applied normal load and the ball size (Fig. 2), which is because of the increase in friction force due to increased contact area.

The contact areas of DLC and SAMs are normally estimated using the Hertzian theory (considering only the first term of Eq. (2), Scherge et al., 2001) as they have lower interfacial energies (indicated by their higher water contact angles (Table 1), Liu et al., 2001. Fig. 10 shows the contact area of Si-wafer calculated using the JKR model (Eq. (2)) and that of DLC using the Hertzian model (only the first term of Eq. (2)). From this figure it could be seen that Si-wafer has higher contact areas when compared to DLC at all loads and ball sizes, which results in higher values of coefficient of friction when compared to DLC (Figs. 2 and 3). In the case of DLC also, the contact area increases with the applied normal load and the ball size. However, the contact area is lower in DLC when compared to Si-wafer, which gives rise to higher contact pressures. This eventually assists the plowing mechanism (Bowden et al., 1950). Further, the plowing component of friction force (F_p) has a direct, but inverse relation with the size of the slider, as seen from Eq. (3) (Bowden et al., 1950). This explains for the decrease in the coefficient of friction with the increase in the ball size in DLC.

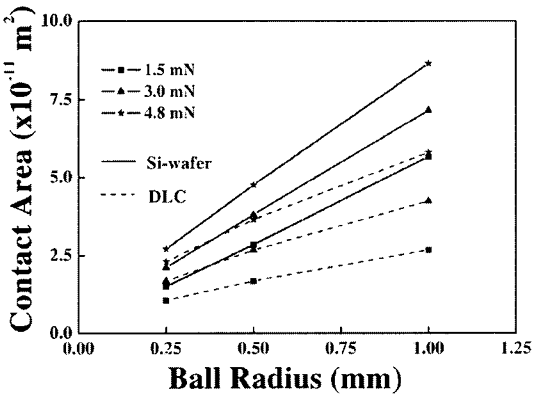

Fig. 10 Contact area of Si-wafer calculated using the JKR model (Eq. (2)) and that of DLC using the Hertzian model (only the first term of Eq. (2))

$$F_p=d^3P/12R \quad (3)$$

where, d is the track width, P the mean pressure required to displace the material in the surface and R the radius of curvature of the slider.

Furthermore, for surfaces making contact at a number of asperities (multiple asperity), the plowing term reduces with the increase in the number of points of contact, for the same load (Bowden et al., 1950). In the present work, under loading conditions in milli-newton (mN) range the contact is not exactly a single asperity contact, but a multiple asperity contact. This also explains for the decrease in the coefficient of friction in the case of DLC with the ball size, and its reduction at higher normal loads.

The friction force in the case of both the SAMs increases with the applied normal load and the ball size, which is due to the increase in the contact area (Eq. (1) and Eq. (2)). Although, the contact area in the case of SAMs could not be calculated (as the values of elastic modulus and Poisson's ratio that are required to calculate the contact area (Eq. (2)) are not readily available nor can they be easily measured), the contact area in the case of SAMs would be much lower when compared to Si-wafer, owing to their lower interfacial energies (indicated by the higher water contact angles (Table 1), Eq. (2)). This would give rise to lower values of friction in the case of the SAMs, which in turn leads to lower values of coefficient of friction in comparison with Si-wafer (Figs. 2, 4 and 5). In addition to lower surface energy, an important feature that reduces friction in SAMs is their molecular chains. These chains exhibit significant freedom of swing and thereby rearrange along the sliding direction under shear stress, which eventually yields a smaller resistance during sliding, thereby exhibiting lower friction (Tupper et al., 1994). Amongst the SAMs, DMDC exhibited better frictional behaviour than DPDC (Figs. 4 and 5). The tribological performance of SAMs depends on several parameters such as their physical properties (chain length and chain stiffness), and chemical properties (composition : head groups and end groups), and coating methods (Bhushan, 2001b ; Oh et al., 2004 ; Singh et al., 2005). In the present case, the increased friction force exhibited by DPDC SAM when compared to DMDC SAM could be mainly due to the higher stiffness of its molecular chain, which is affected by the benzene ring (Bhushan et al., 2001c), when compared to that of the linear chain in DMDC SAM.

In summary, the friction behaviour of Si-wafer, DLC and two different SAMs namely DMDC and DPDC was experimentally investigated under loading conditions in milli-newton (mN) range. It was observed that the occurrence of wear influenced the friction behaviour of Si-wafer and DLC, whereas wear was absent in the case of both the SAMs. The dependence of friction property in the Si-wafer with respect to the ball size (Fig. 2) was indicative that the operating friction mechanism was prominently adhesive in nature. Such an occurrence was due to the solid-solid adhesion that occurred between the Si-wafer and the counterface sliders (as is evident from Figs. 6 and 9(a)). Under such conditions the contact area directly assists the adhesive mechanism. Regarding DLC, the inverse relation of its coefficient of friction with respect to the ball size (Fig. 3) indicated that the operating mechanism was dominated by plowing. Lower contact area assists the plowing mechanism through higher contact pressures. Similar to that in the case of Si-wafer where the friction was influenced by the wear of the material, in the case of DLC too wear influenced its friction property. Unlike in the Si-wafer in which wear occurred by adhesion, DLC undergoes wear by plowing (as is evident from Figs. 7 and 9(b)). The SAMs showed lower values of friction compared to Si-wafer and they exhibited no wear. Thus, indicating that they are good solid lubricants.

4. Conclusions

Friction properties of Si-wafer, DLC, DMDC SAM and DPDC SAM was experimentally evaluated under loading conditions in milli-newton (mN) range. The following are the conclusions drawn from the present work :

(1) Si-wafer exhibited poor frictional property when compared to the rest of the test materials owing to its higher interfacial energy.

(2) Friction was severely influenced by wear in the case of Si-wafer and DLC, whereas the SAMs exhibited no wear. Si-wafer exhibited solid-solid adhesion, while DLC showed plowing.

(3) The coefficient of friction in the case of all the test materials was affected by the ball size. The coefficient of friction increased with the ball size in Si-wafer and the SAMs, whereas in DLC it exhibited an inverse relation owing to its friction mechanism namely, plowing.

(4) SAMs exhibited low friction values when compared to Si-wafer. Their performance was considered to be more superior as they exhibited no wear. Amongst the SAMs, DPDC showed higher friction property than DMDC. This was attributed to its higher stiffness of its molecular chain.

Acknowledgments

This research was supported by a grant (05K 1401-00930) from Center for Nanoscale Mechatronics and Manufacturing of 21st Century Frontier Research Program.

References

Ahmed, S. I., Scherge, M., Li, X. and Schaefer, J. A., 1999, "Microtribological Properties of Self Assembled Monolayers," Proceedings of the GfT-Tribologie-Fachtangung "Reibung, Schmierung und Verschleiss," Gottingen, Germany, pp. 1~8.

Ando, Y. and Ino, J., 1997, "The Effect of Asperity Array Geometry on Friction and Pull-off

Force," *J. Tribol*, Vol. 119, pp. 781~787.

Bhushan, B., 2001b, Modern Tribology Handbook, Vol. 2, CRC Press, Boca Raton, pp. 909~929.

Bhushan, B. and Liu, H., 2001c, "Nanotribological Properties and Mechanisms of Alkylthiol and Biphenyl Thiol Self-assembled Monolayers Studied by AFM," *Physical Review B*, Vol. 63, p. 245412.

Bhushan, B., 1999, "Nanoscale Tribophysics and Tribomechanics," *Wear*, Vol. 225, pp. 465~492.

Bhushan, B., 2001a, "Tribology on the Macroscale to Nanoscale of Micro-electromechanical System Materials," *Proc. Instn. Engrs, ImechE Part J*, Vol. 215, pp. 1~18.

Bowden, F. P. and Tabor, D., 1950, "The Friction and Lubrication of Solids," *Clarendon Press, Oxford*, pp. 90~121.

Eun, K. Y., Lee, K. -R., Yoon, E. -S. and Kong, H., 1996, "Effect of Polymeric Debris on the Tribological Behavior of Diamond-Like Carbon Films," *Surface and Coatings Technology*, Vol. 86~87, pp. 569~574.

Gardos, M. N., 1996, "Surface Chemistry-controlled Tribological Behaviour of Si and Diamond," *Tribology Letters*, Vol. 2, p. 173.

Grischke, M., Hieke, A., Morgenweck, F. and Dimigen, H., 1998, "Variation of the Wettability of DLC-Coatings by Network Modification," *Diamond Related Materials*, Vol. 7, pp. 454~458.

Henck, Steven A., 1997, "Lubrication of Digital Micromirror Devices," *Tribology Letters*, Vol. 3, pp. 239~247.

Johnson, K. L., Kendall, K. and Roberts, A. D., 1971, "Surface Energy and Contact of Elastic Solid," *Proceedings of the Royal Society of London A*, Vol. 324, pp. 301~313.

Komvopoulos, K., 2000, "Head-disk Interface Contact Mechanics for Ultrahigh Density Magnetic Recording," *Wear*, Vol. 238, pp. 1~11.

Lee, K. -R., Eun, K. Y. and Rhee, J. S., 1995, "Structure and Mechanical Properties of Nitrogen Incorporated Diamond-Like Carbon Films," *Mater. Res. Soc. Symp. Proc.*, 356, pp. 233~238.

Liu, H., Ahmed, S. I. -U. and Scherge, M., 2001, "Microtribological Properties of Silicon and Silicon Coated with Diamond Like Carbon, Octadecyltrichlorosilane and Steric Acid Cadmium Salt Films : A Comparative Study," *Thin Solid Films*, Vol. 381, pp. 135~142.

Maboudian, R. and Carraro, C., 2004, "Surface Chemistry and Tribology of MEMS," *Annu. Rev. Phys. Chem*, Vol. 55, pp. 35~54.

Maboudian, R. and Howe, R. T., 1997, "Critical Review : Adhesion in Surface Micromechanical Structure," *J. Vac. Sci. Technol*, Vol. B 15, No. 1, pp. 1~20.

Matweb-Online Material Data Sheet http://www.Matweb.com

Oh, H. -J., Yoon, E. -S., Han, H. -G. and Kong, H., 2004, "Micro/nano Adhesion and Friction Properties of SAMs with Different Head and Functional Group According to the Coating Methods," *KSTLE Spring Conference 2004*, pp. 177~184.

Scherge, M. and Gorb, S. N., 2001, "Biological Micro- and Nanotribology," *Springer-Verlag, Berlin Heidelberg*, pp. 7~76.

Singh, A. R., Yoon, E. -S., Han, H. -G. and Kong, H., 2005, "Friction Characteristics of Self-assembled Monolayers Coated on Si-Wafer by Chemical Vapor Deposition at Nano/Micro-Scale," WTC2005-63417, Micro- and Nanotribology, 3rd World Tribology Congress, Washington D.C, USA, September 2005.

Sundararajan, S. and Bhushan, B., 1999, "Micro/Nanotribology of Ultra-Hard Amorphous Carbon coatings Using Atomic Force/Friction Force Microscopy," *Wear*, Vol. 225, pp. 678~689.

Sundararajan, S. and Bhushan, B., 2001, "Development of a Continuous Microscratch Technique in an Atomic Force Microscope and Its Application to Study Scratch Resistance of Ultrathin Hard Amorphous Carbon Coatings," *J. Mater. Res*, Vol. 16, No. 2, pp. 437~445.

Tupper, K. J. D. and Brenner, W., 1994, "Molecular Dynamics Simulations of Friction in Self-assembled Monolayers," *Thin Solid Films*, Vol. 253, pp. 185~189.

URL: http://www.eetimes.com/story/OEG20010402S0092 "Ohio team studies friction shortfalls of MEMS"

Yoon, E. -S., Kong, H. and Lee, K. -R., 1998, "Tribological Behaviour of Sliding Diamond-like Carbon Films Under Various Environments," *Wear*, Vol. 217, pp. 262~270.

Yoon, E.-S., Yang, S. H., Han, H.-G. and Kong, H., 2003, "An Experimental Study on the Adhesion at a Nano-contact," *Wear*, Vol. 254, pp. 974~980.